Potential of Operational High Spatial Resolution Near-Infrared Remote Sensing Instruments for Snow Surface Type Mapping

Y. Bühler, L. Meier, and C. Ginzler

***Abstract*—Snow changes its morphology permanently from the moment a snow flake touches the ground. Under the influence of meteorological factors such as temperature, humidity, and wind, snow grains form complex structures of ice bonds enclosing variable portions of air. The characteristics of such structures are important for the formation of snow avalanches. Certain snow types such as surface hoar, ice crusts, or windblown snow play a major role in the formation of weak layers and slabs, which are precondition for dangerous slab avalanches. The reflection properties of snow depend on the optical equivalent grain size of the ice particles that constitute the snow cover. High spatial resolution remote sensing instruments with near-infrared (0.7–1.4 μm) bands are able to detect such differences in the optical reflection of snow. We use normalized difference index band ratios from a spaceborne and an airborne remote sensing instrument to distinguish and map different snow-surface types in the neighborhood of Davos, Switzerland, enabling a valuable visualization of the spatial variability of the snow surface.**

***Index Terms*—Near infrared (NIR), optical, snow, snow avalanches, snow grain size.**

I. Introduction

SNOW avalanches have killed people and threatened buildings and infrastructure in alpine terrain since these areas are populated. From the beginning of avalanche research, snow scientists based their findings mainly on measurements at point locations, for example, from snow pits or meteorological stations. However, the alpine snow cover exhibits a high spatial variability in horizontal and vertical directions even on a very small scale mainly caused by the high variability of alpine terrain properties and its influence on wind and radiation [1], [2]. The spatial variability of snowpack properties is important for slab avalanche formation [3], [4] and cannot be properly assessed by point measurements over a wide area.

Remote sensing instruments are capable of acquiring data spatially continuous and over a wide area also covering inaccessible terrain. This is a big advantage for snow research in alpine terrain where data acquisition in the field is often impossible due to avalanche danger or poor accessibility. Therefore, remote sensing instruments have been used to measure and map different snow parameters such as snow-covered area (SCA), fractional snow cover, snow water equivalent, and melting snow on different scales from global [5], [6] to local [7], [8]. In the visible part of the electromagnetic spectrum, snow usually appears white and reflects most of the incoming radiation except if it is polluted by a high portion of sooth or dust [9]. However, in the near-infrared (NIR) part of the spectrum, particularly around a wavelength $\lambda = 1$ μm, the portion of light reflected back to the sensor is highly dependent on the composition of the snowpack surface (Fig. 1). This fact has already been used to measure the optical equivalent grain size of alpine snow surfaces using NIR photography [10] and space- and airborne optoelectronic scanners [11]–[13], demonstrating the potential of optical remote sensing instruments for snow grain size mapping at the surface during cloud-free weather conditions. However, the link between optical equivalent grain size and snow type is not made yet, and no snow-type mapping attempts have been performed. The very high spatial resolutions (0.2–m) of optical sensor systems enable now to see and measure the small-scale spatial variability of snow properties [14].

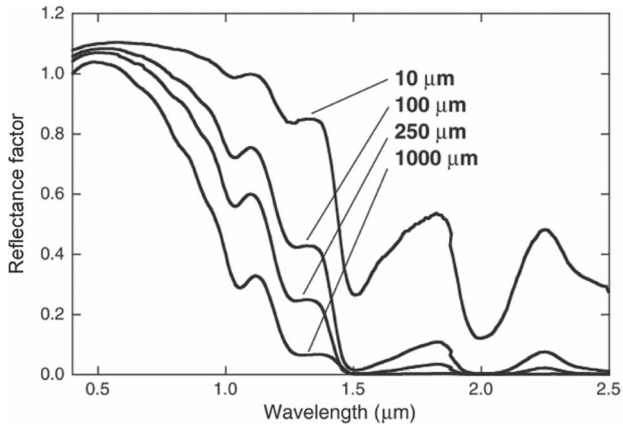

Fig. 1. Reflectance factor of snow dependent on grain size [17].

The optical equivalent grain size can be used as indicator to distinguish between different snow-surface types [15] such as windblown snow, ice crusts, surface hoar, or wet snow. The analysis of snow grain size is an important part of the snow layer characterization in snow profiling [16]. Spatially

Manuscript received January 29, 2014; revised June 4, 2014 and August 26, 2014; accepted October 10, 2014. Date of publication October 29, 2014; date of current version November 20, 2014.

Y. Bühler is with the WSL Institute for Snow and Avalanche Research SLF, 7260 Davos, Switzerland (e-mail: buehler@slf.ch).

L. Meier is with GEOPRAEVENT AG, 8005 Zurich, Switzerland (e-mail: Lorenz.Meier@geopraevent.ch).

C. Ginzler is with the Swiss Federal Institute for Forest, Snow and Landscape Research WSL, 8903 Birmensdorf, Switzerland (e-mail: Christian.ginzler@wsl.ch).

Color versions of one or more of the figures in this paper are available online at http://ieeexplore.ieee.org.

Digital Object Identifier 10.1109/LGRS.2014.2363237

continuous information about the distribution of such snow-surface types over a wide area is valuable information for many applications such as avalanche forecasting, hydrological modeling or the validation of snowpack and wind simulations. In this letter, we demonstrate the potential of air- and spaceborne high spatial resolution remote sensing instruments collecting NIR information to map different snow-surface types in high alpine areas close to Davos, Switzerland.

II. Remote Sensing Instruments and Test Data

To test the potential of NIR remote sensing data for snow-type mapping, we investigate two different sensor systems.

A. WorldView-2

The commercial earth observation satellite WorldView-2 was launched in 2009, operated by DigitalGlobe (http://www.digitalglobe.com). This high spatial resolution sensor [0.5 m panchromatic, 2 m multispectral (MS)] acquires imagery in nine spectral bands, including NIR1 (0.77–0.895 μm) and NIR2 (0.860–1.040 μm). The NIR2 band is of special interest for snow-type mapping covering the electromagnetic spectrum range where the differences in grain size are pictured more distinct (Fig. 1). The test site Davos is located in the eastern part of Switzerland and ranges from elevations of 1500 m at the valley bottom up to 3200 m around the peaks in the southeastern part of the area. The WorldView-2 scene of 10 km by 10 km was acquired on October 30, 2010, at 10:32 A.M. during clear weather conditions with some dust over the valleys. At this time, the snow research season has not yet started, but luckily, there was early snowfall in the area on October 25 and 26 with north–northwestern winds of up to 30 km/h four days before the acquisition of the imagery. The snow cover heights were around 5 cm at the valley bottom and around 25 cm close to the peaks. On October 30, the wind direction changed to south–southwest with speeds of up to 70 km/h. Up to an elevation of 2100 m, the snow cover is not contiguous. We observed a small-scale pattern of snow-free area and SCA with the vegetation cover shining through, typical for the situation after the first snow falls in autumn. Although this situation is not optimal for remote sensing of snow characteristics and differs significantly from the snow cover in winter and spring, we are nevertheless able to use the WorldView-2 data to map different snow types around Davos. The applied orthorectification performed by the data supplier is better than 3.5 m without ground control points.

B. Leica ADS40

The airborne optoelectronic scanner ADS40 is produced by Leica Geosystems. The recent sensor system ADS80 is a further development of the ADS40 system with the same spectral bands. The sensor has a width of 12 000 pixels. The resulting spatial resolution is dependent on the flight height of the airplane above ground and ranges usually between 0.05 and 0.5 m. A detailed description of this sensor is given in [18]. This sensor is capturing data in four spectral bands, including NIR (0.833–0.887 μm). This NIR band is less suitable than the NIR2 of WorldView-2 but still has the potential to differentiate between snow-surface types (Fig. 1). Sensors measuring in this NIR range are integrated in numerous remote sensing instruments on high spatial resolution satellites. On April 26, 2008, between 11:00 and 11:45 local time, an overlapping area in the northwest of Davos was covered by the ADS40 SH52 mounted on a Pilatus-Porter PC6 airplane. The last snowfall before the data acquisition was on April 21, 2008, and the air temperature in the valley was up to 10 °C. Average wind conditions with gust of wind up to 40 km/h mainly from northern direction were present. Due to the strong solar irradiation during the five-day period, since the last snowfall, we can expect a highly variable snow surface. The data acquisition was performed with a mean flight height of 1500 m above ground. This results in an average ground sample distance of 0.20 m. For the data analysis, we resampled the data to 1-m pixel width to be closer to resolutions available from satellite sensors. The radiometric resolution of the 12-b bands was adapted prior to the over flight for the MS bands, reducing saturated areas over snow-covered terrain. This data acquisition was performed to test the avalanche mapping capabilities of this sensor system [18].

III. Methods

A sensor of band i with a relative spectral response $q_i(\lambda)$ will generate a signal proportional to

$$B_i = \int_{-\infty}^{\infty} q_i(\lambda) u_{gs}(\lambda) s(\lambda) d\lambda \tag{1}$$

if looking at an object that has a wavelength-dependent reflectivity $u_{gs}(\lambda)$ (Fig. 1) and reflects light from the sun with an intensity distribution $s(\lambda)$. The incoming solar spectrum includes effects introduced by the atmosphere. This spectrum $s(\lambda)$ is reflected at the snow surface and generates a new spectrum $s'(\lambda) = u_{gs}(\lambda)s(\lambda)$ that is different for varying grain sizes. In the following analysis, we neglect wavelength-dependent effects between the reflection at the snow surface and the detection in the satellite. We assume that these effects are independent of λ and can be divided out using the red channel [19].

To minimize radiometric errors caused by atmospheric conditions and illumination, we use a normalized difference index (NDI), differing out a big part of the atmospheric and illumination effects [20]. By dividing out most illumination effects and atmospheric distortions in the image, this approach allows us to achieve meaningful results without performing radiometric corrections, which are not feasible without a very precise and up-to-date digital surface model (DSM) including the snow cover. Such a DSM is not available. Atmospheric effects are less decisive for the low-flying ADS sensor because there is much less atmosphere between the surface and the sensor compared to satellite-based instruments.

Knowing $q_i(\lambda)$, we can calculate the theoretically expected NDI for the bands $i_{\text{nir}} = 8$(NIR2) and $i_{\text{vis}} = 5$ (red) using the WorldView-2 data (1). For the ADS40/80 sensor, they are $i_{\text{nir}} = 4$ (NIR) and $i_{\text{vis}} = 3$ (red) correspondingly

$$\text{NDI} = \frac{b_{\text{vis}} - b_{\text{nir}}}{b_{\text{vis}} + b_{\text{nir}}}. \tag{2}$$

For four different grain sizes (50, 200, 500, and 1000 μm), the calculated NDIs in the WorldView-2 data are 0.23, 0.17, 0.13, and 0.084, respectively. Thus, there is a pronounced effect that the NDI changes by a factor of almost three when the grain size increases from 50 to 1000 μm. We do not use the blue band from the WorldView-2 satellite because this band has the most atmospheric disturbances. Due to the smaller wavelength of the ADS NIR band and the higher digital number values of the red band, the range of the NDI values of the different snow types changes from 0.15–0.3 (WorldView-2) to 0.4–0.5 (ADS). We expect the differences in the ADS data to be less pronounced but still detectable. We have a variety of snow-surface types due to the longer timespan since the last fresh snowfall. Snow-free and forested areas are masked out using threshold values of the band ratio b_8/b_5 and b_1 (WorldView-2) and b_4/b_3 and b_1 (ADS). These ratios are also used to mask out very thin snowpacks (0–10 cm), where the underlying ground is shimmering through, causing distortion in the NDI signals. Such areas are numerous in the WorldView-2 data acquired after the first major snow fall event in the season.

IV. Results

A. WorldView-2

The NDI map shows areas with high optical equivalent grain size in dark red colors and snow with low values in light blue color. Snow types with large optical equivalent grain size values are mainly wet snow surfaces. The water bonds between snow grains and makes them look like very large grains for the sensors, absorbing a big part of the irradiance in the NIR part of the electromagnetic spectrum [21], [22]. Wind-transported snow, on the other hand, produces very small and spherical grains that form a highly bonded compact snowpack. The small grains of windblown snow reflect significantly more radiation in the NIR than wet snow.

The false-color imagery of the *Jatz* test site (Fig. 2, top), a renowned skiing resort in Davos, makes the dominant role of illumination effects over SCAs obvious. Large parts of the northeast exposed slopes are covered by a cast shadow. Topographic effects caused by the waviness of the terrain lead to brightness differences in the fully illuminated southwest exposed slopes. By applying the NDI (2), we can minimize these illumination effects and make the underlying optical properties of the snow cover visible [19]. The low NDI values on the south exposed slope areas are presumably already wetted snow due to early solar irradiation. To fully prove these assumptions, we would need ground reference data acquired during the over flight of the satellite, which is not available for this data set. No automated weather station measuring snow-surface temperature is available in the area covered by the satellite imagery. Although the ski season starts in mid-November, two weeks after the satellite data were acquired, the preparation of the slopes had already started. By bringing out very small spherical grains using snow guns, a very dense artificial base layer for the ski runs is produced [23]. We can identify the artificially produced snow located trapezoidal around the snow cannons along the future ski runs from the high NDI values, which is an indication of the meaningfulness of the NDI map (Fig. 2, bottom). Owing to the high radiometric resolution of the WorldView-2 sensor (11 b), we can visualize the spatial variability of the snow surface in the cast shadow as well as in the fully illuminated very bright regions.

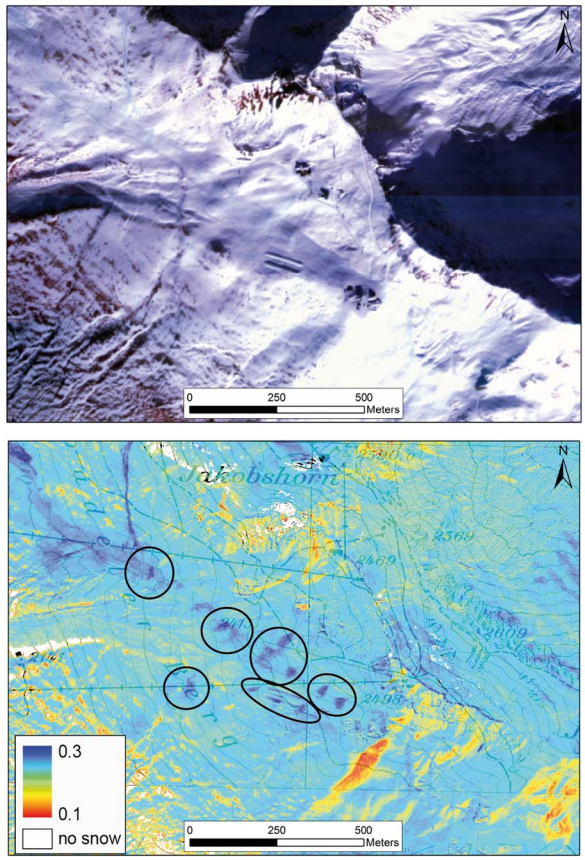

Fig. 2. (Top) False-color image (NIR, red, green) of the sub test site Jatz and (bottom) the corresponding NDI classification on top of the topographic map. (Red) Small NDI values indicate large grain sizes; (blue) high NDI values indicate small grain sizes. Areas of snow cannons are marked with black circles. Topographic map 2013 swisstopo (5704 000 000).

B. Leica ADS40

Even though the NIR band of the ADS sensor is less suitable to distinguish between different optical equivalent grain sizes, we can identify relevant snow-surface types. The high spatial resolution of 0.20 m enables a very detailed view of the spatial variability (Fig. 3). Due to the comparatively long time period since the last snowfall (five days) and the spring conditions (strong solar irradiance and warm temperatures reaching more than 0 °C) we can expect a large variety of snow types in areas of higher elevation (above 2000 m a.s.l.) caused by exposition, topography features (ridges and dells), slope angle, and wind conditions.

We focus on the *Wannengrat* test site, because this area is located at a mountain pass connecting different climatic regions of the canton Graubünden. Here, we find different expositions at high elevation (2400 m a.s.l.) and snow deposition under the influence of high wind speeds. Fig. 3 demonstrates the potential of the NDI differing out illumination and atmospheric effects and making different snow types visible.

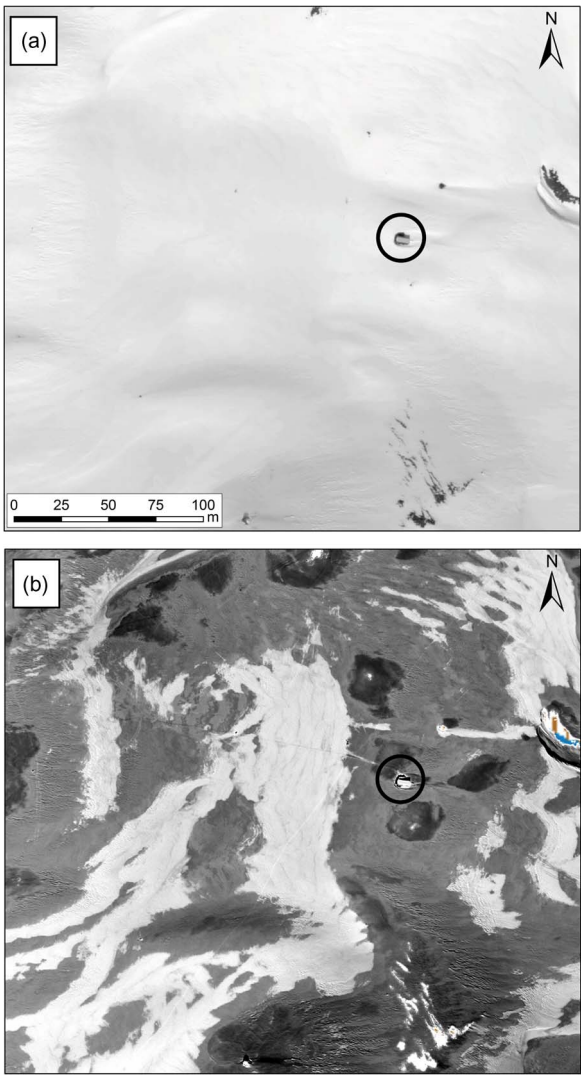

Fig. 3. (A) Red band (0.608–0.662 μm). (B) NDI (2) of the Wannengrat sub test site; the NDI values range from (black) 0.4 to (white) 0.5. The hut described in the text for better orientation is marked with a black circle.

The southeast exposed slopes of the two small hills north and south of the hut appear as dark areas in the NDI image. This corresponds to very large optical equivalent grain sizes produced by free water melting at the snow surface due to the high solar irradiation. The bright area west of the hut corresponds to small optical equivalent grain sizes. We assume that this snow was deposited by strong winds from the northwest (the dominant wind regime in this area) that deposits eroded snow grains behind the ridge. We can also identify rough snow surfaces formed by wind erosion at the southern and western edges of the image.

C. Comparison With Field Observations

For the two presented data acquisitions (WV-2 and ADS40), no field reference data are available. However, on March 31, 2009, a field campaign was organized, measuring surface grain size at the ground simultaneously to an ADS40 over flight performed by SLF field staff at 23 locations with varying elevations and expositions. The filed campaign is described in detail in [24]. However, measuring small grain sizes by eye on a scale

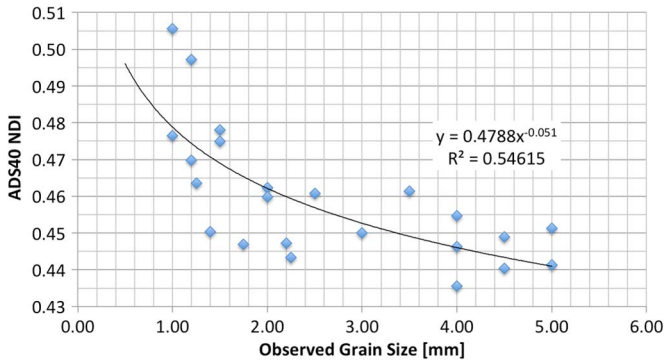

Fig. 4. Correlation between measured snow grain size and ADS40 NDI values acquired on March 31, 2009.

is a difficult task; biases between different observers may occur, and only a limited accuracy can be achieved. In addition, it snowed until the evening before the over flight, and the entire surface was covered by a comparably homogeneous new snow cover. Therefore, the measured range of snow-surface grain size is limited to 4 mm. However, these field observations demonstrate the logarithmic correlation between measured grain size and NDI values (Fig. 4).

V. Conclusion

Even though we only have limited field observations available for this study, we can demonstrate the potential of MS high spatial resolution remote sensing imagery for snow-type mapping in high alpine terrain. The WorldView-2 satellite imagery was acquired in autumn under suboptimal snow conditions. However, we are able to identify different snow types by mapping the NDI. The additional NIR2 band of the WorldView-2 sensors, measuring the reflected irradiance in wavelengths between 0.860 and 1.040 μm, is an advantage for remote sensing of SCAs. Theoretically, it is capable of differentiating between optical equivalent grain sizes [21]. These grain sizes are a suitable indicator to identify different snow types such as windblown snow, ice crusts, and wet snow surfaces. This is supported by the clear identifiability of artificial snow in Fig. 2.

The airborne ADS40 sensor with its very high spatial resolution of 0.2 m also proves to be a useful instrument for snow-type mapping, even though the NIR band measures in the shorter wavelength range of 0.833–0.887 μm, where the effect of optical equivalent grain sizes on reflectance is less distinct (Fig. 1). We can support this statement by comparing field-measured grain sizes with the NDI values of an ADS40 data acquisition (Fig. 4).

Today, numerous air- and spaceborne instruments with NIR bands are operationally in use. This enhances the data availability for any given test site substantially. By using an NDI of two different bands, we can reduce the overlying illumination and atmospheric effects. We have shown the potential to identify artificial snow, wet snow, and windblown snow even in poorly accessible terrain. This is valuable information for avalanche forecasting, snow hydrology, and further snow-related research. Owing to the high radiometric resolution of 10–16 b, these sensors are able to derive information even in cast-shadow-covered areas, which is a big advantage in steep alpine terrain.

However, to exactly map grain sizes with optical remote sensing instruments, an accurate atmospheric and radiometric correction, as well as an absolute calibration of the instruments, would be necessary [25]. In addition, reference measurements of a larger range of grain sizes are needed. It is difficult to get enough samples of different snow types within a large area mainly because the snow surface can change within minutes under spring conditions. Using snowpack models such as Alpine3D [26] to verify the snow-type classification makes no sense in our opinion because these models cannot capture the small-scale spatial variability that we find in the NDI images. The finest resolution for Alpine3D is 25 m, which results in 10 000 pixel values in the ADS80 data set with 0.25-m spatial resolution. Therefore, the presented approach is more suitable for qualitative mapping of different snow-surface types in combination with expert knowledge rather than for a strict grain size mapping.

Optical remote sensing data can only be acquired under cloud-free conditions and during daytime. This constraint is not present for active radar instruments such as SAR. However, the interaction of radar waves with snow is not yet understood sufficiently to reliably map snow-surface types, and fewer operational sensors are available with high spatial resolution. We are confident that future high spatial resolution remote sensing studies including sufficient field measurements are able to reveal valuable new findings on the spatial distribution of snow types and those operational remote sensing instruments will be used more frequently for snow-related studies.

ACKNOWLEDGMENT

The authors would like to thank Leica Geosystems and DigitalGlobe for the provision of the remote sensing data and the in-house staff of SLF for the support in the remote sensing investigations.

REFERENCES

[1] L. Egli and T. Jonas, "Hysteretic dynamics of seasonal snow depth distribution in the Swiss Alps," *Geophys. Res. Lett.*, vol. 36, no. 2, pp. L02501-1–L02501-5, Jan. 2009.

[2] M. Lehning, H. Löwe, M. Ryser, and N. Raderschall, "Inhomogeneous precipitation distribution and snow transport in steep terrain," *Water Resources Res.*, vol. 44, no. 7, pp. W07404-1–W07404-19, Jul. 2008.

[3] K. Birkeland, "Spatial patterns of snow stability throughout a small mountain range," *J. Glaciol.*, vol. 47, no. 157, pp. 176–186, 2001.

[4] J. Schweizer, K. Kronholm, J.B. Jamieson, and K.W. Birkeland, "Review of spatial variability of snowpack properties and its importance for avalanche formation," *Cold Regions Sci. Technol.*, vol. 51, no. 2/3, pp. 253–272, Feb. 2008.

[5] A. Dietz, C. Kuenzer, U. Gessner, and S. Dech, "Remote sensing of snow—A review of available methods," *Int. J. Remote Sens.*, vol. 33, no. 13, pp. 4094–4134, 2012.

[6] G.W. Rees, *Remote Sensing of Snow and Ice*. Boca Raton, USA: CRC Press, 2006.

[7] A. Nolin, "Recent advances in remote sensing of seasonal snow," *J. Glaciology*, vol. 56, no. 200, pp. 1141–1150, 2010.

[8] J. Dozier and T. H. Painter, "Multispectral and hyperspectral remote sensing of alpine snow properties," *Annu. Rev. Earth Planetary Sci.*, vol. 32, pp. 465–494, May 2004.

[9] S. Warren and W. Wiscombe, "A Model for the Spectral Albedo of Snow. II: Snow Containing Atmospheric Aerosols," *J. Atmos. Sci.*, vol. 37, no. 12, pp. 2734–2745, Dec. 1980.

[10] M. Matzl and M. Schneebeli, "Measuring specific surface area of snow by near-infrared photography," *J. Glaciol.*, vol. 52, no. 179, pp. 558–564, Dec. 2006.

[11] A. W. Nolin and J. Dozier, "A hyperspectral method for remotely sensing the grain size of snow," *Remote Sens. Environ.*, vol. 74, no. 2, pp. 207–216, Nov. 2000.

[12] T. Tanikawa, T. Aoki, and F. Nishio, "Remote sensing of snow grain-size and impurities from airborne multispectral scanner data using a snow bidirectional reflectance distribution function model," *Ann. Glaciol.*, vol. 34, no. 1, pp. 74–80, Jan. 2002.

[13] J. Dozier, R. O. Green, A. W. Nolin, and T. H. Painter, "Interpretation of snow properties from imaging spectrometry," *Remote Sens. Environ.*, vol. 113, pp. 25–37, 2009.

[14] Y. Bühler, "Remote sensing tools for snow and avalanche research," in *Proc. ISSW*, Anchorage, AK, USA, 2012, pp. 264–268.

[15] C. Fierz *et al.*, *The International Classification for Seasonal Snow on the Ground*. Paris, France: United Nations Educ., Sci. and Cultural Org. (UNESCO-IHP), 2009. [Online]. Available: http://www.cryosphericsciences.org/snowClassification.html

[16] J. Schweizer and J. Jamieson, "Snowpack properties for snow profile analysis," *Cold Regions Sci. Technol.*, vol. 37, pp. 233–241, 2003.

[17] T. H. Painter, J. Dozier, D. A. Roberts, R. E. Davis, and R. O. Green, "Retrieval of subpixel snow-covered area and grain size from imaging spectrometer data," *Remote Sens. Environ.*, vol. 85, pp. 64–77, 2003.

[18] Y. Bühler, A. Hüni, M. Christen, R. Meister, and T. Kellenberger, "Automated detection and mapping of avalanche deposits using airborne optical remote sensing data," *Cold Regions Sci. Technol.*, vol. 57, no. 2/3, pp. 99–106, Jul. 2009.

[19] J. K. Shultis, "Calculated sensitivities of several optical radiometric indices for vegetation canopies," *Remote Sen. Environ.*, vol. 38, no. 3, pp. 211–228, 1991.

[20] H. R. Gordon, "Removal of atmospheric effects from satellite imagery of the oceans," *Appl. Opt.*, vol. 17, no. 10, pp. 1631–1636, May 1978.

[21] S. Warren, "Optical properties of snow," *Rev. Geophys. Space Phys.*, vol. 20, no. 1, pp. 67–89, Feb. 1982.

[22] T. Painter, N. Molotch, M. Cassidy, M. Flanner, and K. Steffen, "Instruments and methods: Contact spectroscopy for determination of stratigraphy of snow optical grain size," *J. Glaciol.*, vol. 53, no. 180, pp. 121–127, 2007.

[23] S. Wipf, C. Rixen, M. Fischer, B. Schmid, and V. Stoeckli, "Effects of ski piste preparation on alpine vegetation," *J. Appl. Ecol.*, vol. 42, no. 2, pp. 306–316, Apr. 2005.

[24] G. Raymann, "Kartierung der Kleinräumigen Variation von Schneeoberflächen," M.Sc. thesis, Remote Sensing Laboratories, Univ. Zurich, Zurich, Switzerland, 2010, (German).

[25] R. Richter, D. Schläpfer, and A. Mueller, "An automatic atmospheric correction algorithm for visible/NIR imagery," *Int. J. Remote Sens.*, vol. 27, no. 10, pp. 2077–2085, 2006.

[26] M. Lehning *et al.*, "ALPINE3D: A detailed model of mountain surface processes and its application to snow hydrology," *Hydrol. Proces.*, vol. 20, no. 10, pp. 2111–2128, Jun. 2006.